

# Squid-Inspired Smart Window by Movement of Magnetic Nanoparticles in Asymmetric Confinement

Junseok Yang, Hyunggyu Lee, Seong Gil Heo, Sunghwan Kang, Hyemin Lee, Cho Hee Lee, and Hyunsik Yoon\*

The camouflage used by cephalopods is an interesting topic in biomimetics. Squid, part of the cephalopod family, have transformable skin that can be made transparent or darkened through control of the light-absorption area. This is achieved using a muscular structure. A smart-window scheme inspired by this is developed. Magnetic nanopigments dispersed within an asymmetric pyramidal array are used and the light-absorption area is manipulated through use of a magnetic field. Refractive-index-matched liquids are used as a dispersion media to avoid refraction at the interface. The transparency hysteresis (ON/OFF ratio) performance depends on the ratio of magnetic nanoparticles and the dispersive fluid and a model is derived to explain this. In addition, a 3D-printed structure is proposed and demonstrated for better performance.

Many creatures, such as chameleons, insects, and cephalopods, are capable of adapting to their surroundings to protect or disguise their bodies.<sup>[1]</sup> A chameleon has the ability to change color for camouflage or communication by actively tuning the structural medium or multilayers to generate light interference.<sup>[2,3]</sup> To be inspired from the camouflage of the animals, Whitesides et al. proposed a concept of fabricating soft machines from microfluidic devices to generate camouflaged colors by pumping colored fluids into the microfluidic channels.<sup>[1]</sup> Bao et al. extended the idea of color change for an electronic skin by combining this change with tactile sensing.<sup>[2]</sup> Recently, cephalopods have received attention for the functions that allow disguise.<sup>[4]</sup> They can alter their transparency as well as control colors. This occurs through the action of thousands

of chromatophores, which are pigmented organs. Light is reflected by the chromatophores, which consist of pigment-containing sacs. By controlling the muscles attached to their surroundings, cephalopods such as squids can manipulate their skin's transparency.<sup>[4-9]</sup> Inspired by the camouflage of cephalopods, there have been several studies of mimicking this ability.<sup>[5-9]</sup> Sun et al. reported a deformation-controlled method to harness mechano-chromisms by using optical design.<sup>[5]</sup> Wang et al. showed an electro-mechano-chemical response of elastomers by using electric fields.<sup>[6]</sup> Yu et al. demonstrated the adaptive system inspired from cephalopods with thermochromic


materials,<sup>[7]</sup> and Rossiter et al. used the actuation with dielectric elastomers to be used as an artificial muscle to modulate the transmittance.<sup>[8]</sup> Although they demonstrated possible applications for new types of display devices, complex fabrication schemes or mechanical signals would be needed. In particular, it is difficult to mimic the behavior of the muscles on the sacs in order to control the light absorbent area of the pigments within the sacs. Herein, we propose a simple method to manipulate the light absorption area by moving pigments within asymmetric structures such as pyramids to change the transparency. Magnetic nanoparticles are used as pigments to absorb light, and they move in the confined asymmetric medium. We exploited the refractive index matching of liquids and transparent polymeric structures to avoid refraction at their interface. We control the hysteresis of transparency (ON/OFF ratio) by manipulating the ratio of magnetic particles to the disperse media. Furthermore, we designed a structure for better On/Off ratio and demonstrated this by using 3D printing methods. This function could be used for smart windows, which can tune the transmittance of the window.

**Figure 1a** is a schematic illustration explaining the mechanism of the transparency change in the skin of squid. A squid has chromatophores containing melanin pigments, which absorb light. When the pigments aggregate, the area of the transparent region is increased. Conversely, when the pigments are spread out, the area that absorbs light is increased, and the skin is not transparent.<sup>[4]</sup> In a squid, a muscle contracts and promotes release of the pigment, causing the changes in the transparency and opacity of the skin. In the ideal case, the pigments should spread and condense in two dimensions. However, there are few reports to mimic this behavior. We use a 3D design to

J. Yang, H. Lee, S. Kang, C. H. Lee, Prof. H. Yoon  
Department of Chemical and Biomolecular Engineering  
Seoul National University of Science & Technology  
Seoul 01811, Korea  
E-mail: hsyoon@seoultech.ac.kr

S. G. Heo, H. Lee, Prof. H. Yoon  
Department of New Energy Engineering  
Seoul National University of Science & Technology  
Seoul 01811, Korea

S. G. Heo, Prof. H. Yoon  
3D EYES  
131-1 Second Business Incubation Center  
Seoul National University of Science & Technology  
Seoul 01811, Korea

 The ORCID identification number(s) for the author(s) of this article can be found under <https://doi.org/10.1002/admt.201900140>.

DOI: 10.1002/admt.201900140

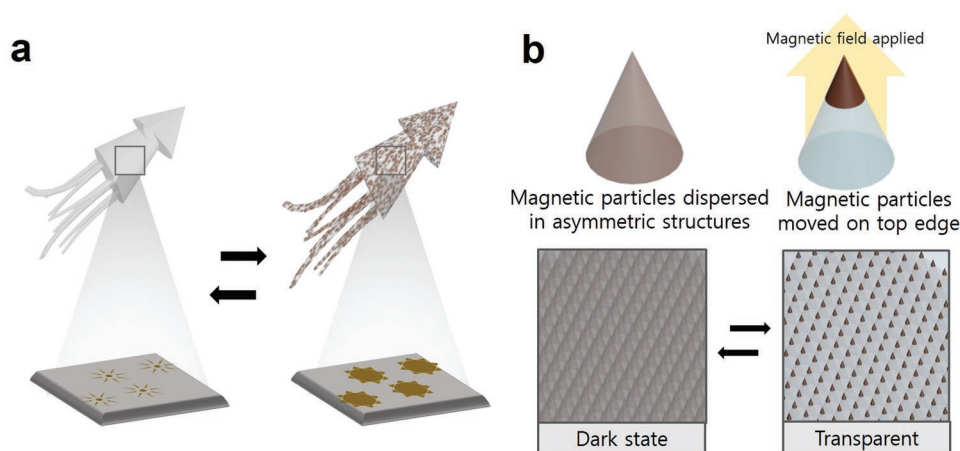


**Figure 1.** a) A schematic illustration representing the mechanism of the transparency change of squid skin. b) A 3D design to control light absorption area by pigment.

control the area in which light is absorbed by the pigment by magnetic field, as shown in Figure 1b. To realize this concept, we design and fabricate structures of pyramid arrays and then filled them with a liquid dispersed by magnetic particles. When a magnetic field was applied in the direction of the apexes of the pyramids, the magnetic particles aggregated in a small area of light absorption; however, when the magnetic field is not applied or is applied to the bottom of the pyramids, the magnetic particles dispersed or moved toward the bottom of the pyramids, then the area of light absorption is increased, thus, the total area becomes dark.

Based on the idea of exploiting 3D structures, here we demonstrate the concept of controlling the light absorption area, as shown in Figure 2. First, we fabricated 3D master patterns by using stereolithographic 3D printing methods. We use a commercial 3D printer (LITHO, Illuminade Co., Ltd.), in which programmed 3D patterns are generated by digital light processing with a lamp power of 190 W, and the exposure dose of 8–12 W m<sup>-2</sup>. Designed 3D structures by a software (3DS Max) can be converted to many 2D patterns for 3D printing. We use the UV curable resin provided by the 3D printer company (LITHO, Illuminade Co., Ltd.). After preparing the master patterns by the 3D printer, we replicate the negative patterns using polydimethylsiloxane (PDMS). To release the PDMS from the master mold, first, we treat the master by fluorinated self-assembled monolayer on the surface to form an antisticking surface. Then, we poured the mixture of PDMS prepolymer and curing agent (10:1 ratio) onto the master, followed by thermal crosslinking at 60 °C for more than 4 h. The detached PDMS patterns had the shape of an inverse pyramid. Figure S1 in the Supporting Information shows the detail experimental procedure. Figure 2a illustrates the process wherein we placed the PDMS onto a paper printing university logo. Although the PDMS was transparent enough, the surface was opaque because of the refraction on the interface of the pyramidal structures. To remove the scattering effect, we filled it with liquid of the same refractive index as PDMS (1.41). In this experiment, we used a mixture (0.485:0.515) of polyethylene glycol (PEG) and isopropyl alcohol (IPA) to match the refractive index. After matching the refractive index, the PDMS pattern covered with a liquid was transparent without any refraction,

as shown in Figure 2b. To absorb the light, we prepared iron oxide (III) (Fe<sub>2</sub>O<sub>3</sub>) nanoparticles with an average particle size of 50 nm or less or purchased from Sigma-Aldrich and dispersed in the refractive index-matched liquid. When the nanoparticle-dispersed liquid is filled into the void of the PDMS, as shown in Figure 2c, the entire area was opaque due to the light absorption by the magnetic nanoparticles. When the magnetic field was applied in the upper direction, as shown in Figure 2d, the magnetic nanoparticles aggregated in the apex area, and the light absorbing area was reduced. Thus, the transparent area was increased.

To control the hysteresis of the transparency and opacity, we controlled the concentration of magnetic particles that were dispersed in the refractive index-matched liquid. As shown in Figure 3a, incident light can be transmitted, even in the dispersed state (OFF state), when the concentration of magnetic particles is 0.05 weight (wt)%. Although the transmittance was high when the magnetic field was applied (ON state), the transmittance difference is not sufficient to be distinguished. When we increased the concentration of magnetic nanoparticles to 0.5 wt%, the window became dark in the OFF state, and the transmittance was high enough to see the university logo through the window in the ON state (Figure 3b). When the concentration of magnetic particles was too high (2 wt%), however, the transmittance in the ON state could be reduced. For the quantitative study, we measured luminance of display panel through the films filled with magnetic nanoparticles by using a commercial luminance light digital meter (Sunche, hs1010A) as shown in Figure 3b. To analyze the experimental data, we used a simple model for the transmittance in the ON/OFF state depending on the concentration of magnetic particles. In the ON state, the transmittance ( $T_{\text{ON}}$ ) can be derived as

$$T_{\text{ON}} \sim 1 - \left(\frac{x}{L}\right)^2 \quad (1)$$

where  $x$  is the width of the bottom of the pyramid consisting of magnetic particles and  $L$  is the width of the bottom of the pyramidal structures (Figure S2, Supporting Information). We

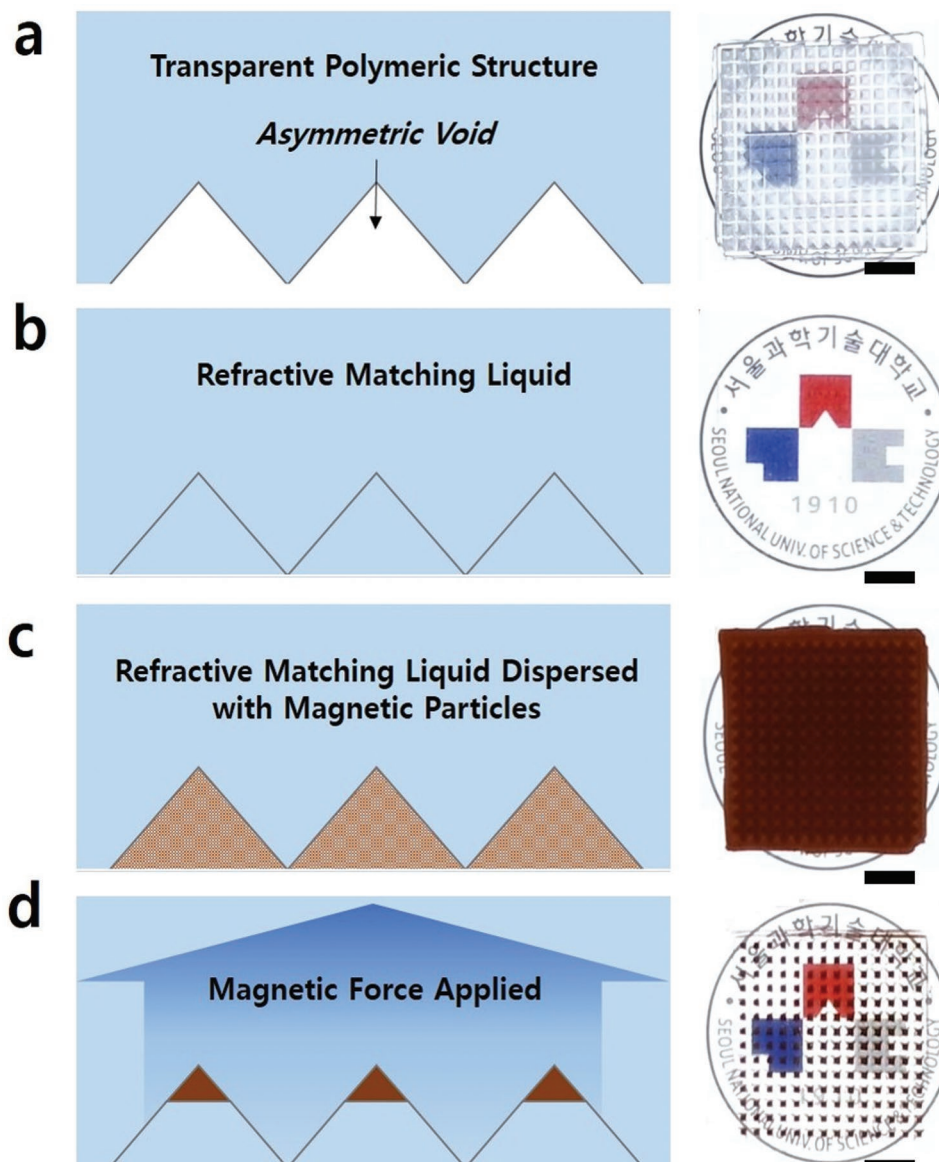


**Figure 2.** Schematic illustrations and images a) when a PDMS pyramidal array is placed on a university logo printed in a paper, b) the PDMS array is filled by a refractive index–matched liquid, c) magnetic particles are dispersed in the refractive index–matched liquid, and d) magnetic particles move to the apex area of the pyramidal structures. Scale bars represent 1 cm.

assumed that the magnetic particles can absorb incident light completely when the magnetic particles are gathered in the apex of the pyramids. The volume ratio of the magnetic particles is  $(x/L)^3$ . When we convert the volume ratio to the weight ratio  $r$ , the relation is as follows

$$\rho \left( \frac{x}{L} \right)^3 = r \quad (2)$$

where  $\rho$  is the packing density of the magnetic particles. Then, we can obtain the relation between the transmittance and the weight ratio ( $r$ ) of the magnetic particles

$$T_{\text{ON}} \sim 1 - Ar^{2/3} \quad (3)$$

where  $A$  corresponds to  $(1/\rho)^{2/3}$ . In the OFF state, the transmittance can be predicted by the Beer–Lambert law<sup>[10]</sup>

$$T_{\text{OFF}} = \exp(-\alpha\delta) \quad (4)$$

where  $\alpha$  is the absorption coefficient and  $\delta$  is the thickness of the absorbent. When we assume the particles are lying on the bottom side in small thickness uniformly, and the volume of the thickness is the same with the volume gathered into the apex region, we can derive the relation as below

$$\delta L^2 = \frac{1}{3} x^2 h, \quad \delta = \frac{h}{3} \left( \frac{x}{L} \right)^2 \sim \frac{H}{3} \left( \frac{x}{L} \right)^3 \sim \frac{H}{3} \frac{r}{\rho} \quad (5)$$

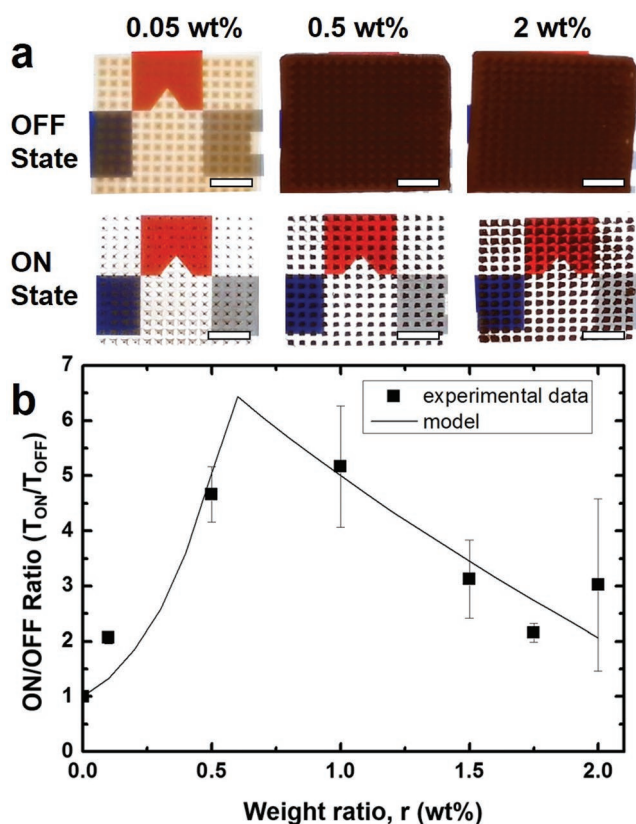


**Figure 3.** a) Transparency of films incorporating magnetic nanoparticles in different weight percent of nanoparticles. We place the film on a screen of a display panel. ON and OFF states mean that there is applying magnetic field or not. Scale bars represent 1 cm. b) A graph showing ON/OFF ratios from the experimental data of the luminance measurement by a commercial light meter and  $T_{ON}/T_{OFF}$  derived in a supposed model.

where  $H$  is the height of the prism. When we combine Equations (4) and (5), the transmittance in off state can be given by

$$T_{OFF} = \exp(-Br) \quad (6)$$

where  $B = \alpha H/3\rho$ . Because there was a light leak during the measurement (Figure S4, Supporting Information), we set to 10% as the minimum transmittance in the model, in case the calculated transmittance is smaller than 10%. We note that the calculated transmittance when the weight ratio is 0.5 wt% is 0.13 and it is invisible as shown in Figure 3a. The maximum point of Figure 3b is due to the minimum setting. From the fitting of the model in Figure 3b, we obtained the packing density of nanoparticles ( $\rho = 0.0283$ ) and the absorption coefficient ( $\alpha = 17 \text{ mm}^{-1}$ ). It means the nanoparticles are not closely packed even when they are attracted to the apex area by the magnetic field because the nanoparticles are surrounded by the fluid mixture (PEG and IPA). For example, we can estimate the volumetric ratio of light absorption by magnetic particles to 35.3% when the weight ratio is only 1%. Also, we can estimate the thickness of the nanoparticles (1.5  $\mu\text{m}$ ) to reduce the transmittance to 0.5 ( $B = 0.3$  and  $r = 1$  in Equation (6)) from the absorption coefficient, which is another effect of low packing density of nanoparticles. It takes 1 min to be ON state during

applying a magnetic field and several seconds to be dispersed with a slight agitation with the magnet. When we use larger particles of carbonyl iron powder (3–10  $\mu\text{m}$ , Chemical Store Inc., USA), the response time became faster (a few seconds).

For better performance of ON/OFF ratio, we tuned the structures. To increase the luminance in the ON state, we designed hopper-like structures by a graphic software, as shown in Figure 4a and Figure S3 in the Supporting Information. In comparison with the pyramidal structures, the absorption area can be reduced to  $\pi r^2$ , which is the area of circular structures. Instead, we made pillar structures to collect the nanoparticles within a small area. To demonstrate this concept, we fabricated the hopper structures using a 3D printing method. In our experiment, we used a stereolithographic 3D printer that can produce structures with high resolution. Figure 4b shows an image of a hopper array fabricated by a 3D printer. After replica molding, we can obtain an inversed structure with PDMS, as shown in Figure 4c. Figure 4d,e shows the side schematic comparison of the ON/OFF states with pyramidal structures and hopper structures. In the ON state, Figure 4e with top-shaped pillar structures can be filled with the magnetic nanoparticles in the pillar. The experimental results in Figure 4f,g for the two different structures show when the magnetic field was applied (ON state), the university logo and name of the hopper structures in Figure 4g can be seen more clearly than pyramidal structures of Figure 4f because the hopper structures can reduce the light-screening area. The transmittance of the hopper array is 50% higher than that of the pyramidal structure (weight ratio: 0.5 wt%) as shown in Figure S5 in the Supporting Information.

It is notable to compare our method to conventional methods. Smart windows can change transmission of radiation in the solar spectrum and they have received much attention due to the possibility of reduction of energy consumption.<sup>[11–14]</sup> In the smart windows, there are two categories. One is the passive methods using photochromic and thermochromic methods. In this case, the transparency can be automatically controllable but it is impossible to manipulate by manual. The other is active methods using electric signals. In this case, smart windows can be fabricated with electrochromic materials or liquid crystals and suspended particles.<sup>[14]</sup> Our method is similar to the suspended particles devices (SPDs). However, in our method, we exploit the guide of the movement of suspended particles within directionally guided void arrays, which is totally different with SPD using alignment of particles in the solvent. Recently, there have been several reports to use magnetic field to tune the surface morphology, however, the movement of the magnetic nanoparticles within the refractive index-matched fluid is convenient to control without the refraction caused by the microstructures.<sup>[15,16]</sup>

In summary, we proposed a squid-inspired method for a smart window. By directional guidance of magnetic field by asymmetric structures, we could manipulate the light absorption area with magnetic field. Furthermore, we designed the more efficient structures for maximizing the ON/OFF ratio. The structures can be adapted for future display devices.

## Experimental Section

**Preparation of Polymeric Structures:** The pyramidal structures were designed by a computer aided design (CAD) program and the



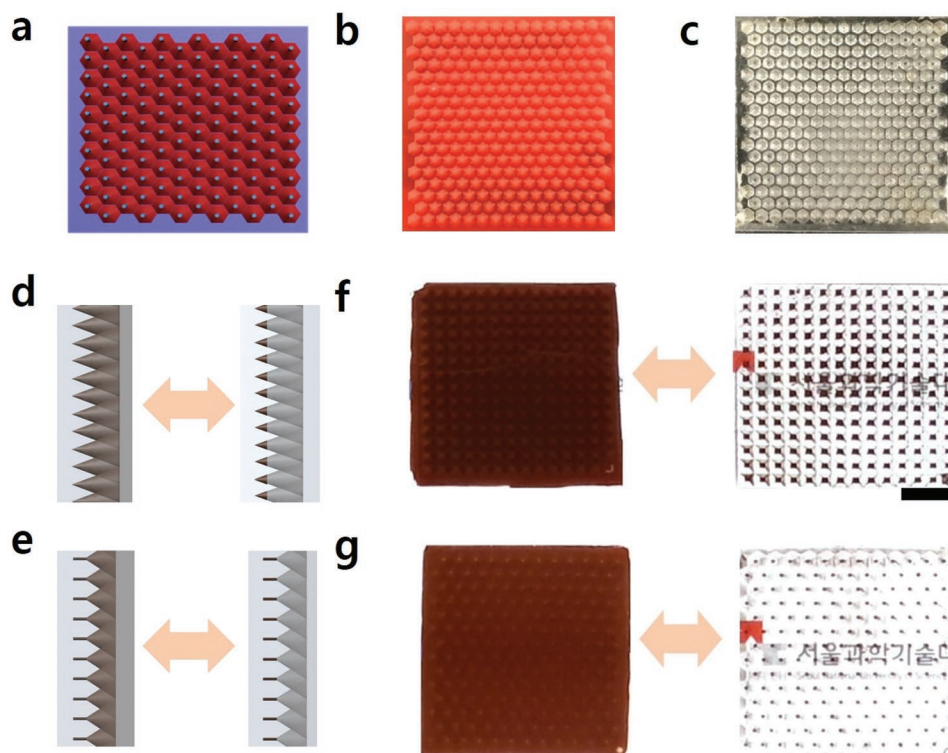


**Figure 4.** Better luminance performance of smart windows with a) designed hopper-like structures by a software (3DS Max), b) the hopper structure by a 3D printer, c) a PDMS inverse pattern, d,e) the side schematic comparison of the ON/OFF states with pyramidal structures and hopper structures, and f,g) experimental results with two different structures. The scale bars represent 1 cm.

polymeric structures were fabricated by mechanical machining or stereolithographic 3D printing (Illuminade). After preparing masters, a liquid mixture of PDMS prepolymer with curing agent was poured onto the master. The mixing ratio was 10:1. After crosslinking for 4 h, the PDMS structure was detached from the master by a peeling method.

**Magnetic Particles Dispersed in Refractive Index Matching Liquid:** Iron oxide (III) ( $\text{Fe}_2\text{O}_3$ ) nanoparticles with an average particle size of 50 nm or less were purchased from Sigma-Aldrich. Refractive index matching liquid was prepared by mixing IPA and PEG (PEG molecular weight = 300, Sigma Aldrich) with a ratio of 0.485:0.515 and the refractive index was tuned to 1.41, which was that of PDMS. After adding magnetic nanoparticles in the liquid, ultra-sonication was done for the dispersion.

**Switching Transmittance by Magnetic Field:** When the magnetic particles were attracted to the bottom, the absorption area was increased. A neodymium magnet (N42, surface magnetic field = 3605 Gauss) was placed to drag the magnetic nanoparticles. When the magnetic particles were gathered in apex area, the absorption area became small then it could be transparent. To compare the performance of smart windows, the luminance was measured by a photodetector (Tasi-8721) through the films. In addition, a window tint meter (AT-173, Guangzhou Amittari Instruments Co., Ltd.) was used to measure the transmittance.

## Supporting Information

Supporting Information is available from the Wiley Online Library or from the author.

## Acknowledgements

J.Y., H.L., and S.G.H. contributed equally to this work. This work was supported by Seoul National University of Science & Technology, the

National Research Foundation of Korea (NRF) grant funded by the Korea government (MEST) (2016R1A2B4013640), and the Commercialization Promotion Agency for R&D Outcomes Grant funded by the Korean Government (MSIP) (2015, Joint Research Corporations Support Program), and LG Yonam Foundation (of Korea).

## Conflict of Interest

The authors declare no conflict of interest.

## Keywords

3D printing, biomimetics, nanoparticles, smart windows

Received: February 14, 2019

Revised: April 24, 2019

Published online:

- [1] S. A. Morin, R. F. Shepherd, S. W. Kwok, A. A. Stokes, A. Nemiroski, G. M. Whitesides, *Science* **2012**, *337*, 828.
- [2] H.-H. Chou, A. Nguyen, A. Chortos, J. W. F. To, C. Lu, J. Mei, T. Kurosawa, W.-G. Bae, J. B.-H. Tok, Z. Bao, *Nat. Commun.* **2015**, *6*, 8011.
- [3] J. Teyssier, S. V. Saenko, D. van der Marel, M. C. Milinkovitch, *Nat. Commun.* **2015**, *6*, 6368.
- [4] L. M. Mähger, E. J. Denton, N. J. Marshall, R. T. Hanlon, *J. R. Soc., Interface* **2009**, *6*, S149.

- [5] S. Zeng, D. Zhang, W. Huang, Z. Wang, S. G. Freire, X. Yu, A. T. Smith, E. Y. Huang, H. Nguon, L. Sun, *Nat. Commun.* **2016**, *7*, 11802.
- [6] S. Wang, G. R. Gossweiler, S. L. Craig, X. Zhao, *Nat. Commun.* **2014**, *5*, 48999.
- [7] C. Yu, Y. Li, X. Zhang, X. Huang, V. Malyarchuk, S. Wang, Y. Shi, L. Gao, Y. Su, Y. Zhang, H. Xu, R. T. Hanlon, Y. Huang, J. A. Rogers, *Proc. Natl. Acad. Sci. U. S. A.* **2014**, *111*, 12998.
- [8] J. Rossiter, B. Yap, A. Conn, *Bioinspiration Biomimetics* **2012**, *7*, 036009.
- [9] L. Phan, W. G. Walkup IV, D. D. Ordinario, E. Karshalev, J.-M. Jocsion, A. M. Burke, A. A. Gorodetsky, *Adv. Mater.* **2013**, *25*, 5621.
- [10] F. L. Pedrotti, L. M. Pedrotti, L. S. Pedrotti, *Introduction to Optics*, 3rd ed., Pearson/Prentice Hall, Englewood Cliffs, NJ **2007**.
- [11] M. P. Gutierrez, L. P. Lee, *Science* **2013**, *341*, 247.
- [12] C. Bechinger, S. Ferrere, A. Zaban, J. Sprague, B. A. Gregg, *Nature* **1996**, *383*, 608.
- [13] H.-K. Kwon, K.-T. Lee, K. Hur, S. H. Moon, M. M. Quasim, T. D. Wilkinson, J.-Y. Han, H. Ko, I.-K. Han, B. Park, B. K. Min, B.-K. Ju, S. M. Morris, R. H. Friend, D.-H. Ko, *Adv. Energy Mater.* **2014**, *5*, 1401347.
- [14] R. Baetens, B. P. Jelle, A. Gustavsen, *Sol. Energy Mater. Sol. Cells* **2010**, *94*, 87.
- [15] Y. Zhu, D. S. Antao, R. Xiao, E. N. Wang, *Adv. Mater.* **2014**, *26*, 6442.
- [16] J. H. Kim, S. M. Kang, B. J. Lee, H. Ko, W.-G. Bae, K. Y. Suh, M. K. Kwak, H. E. Jeong, *Sci. Rep.* **2016**, *5*, 17843.